First experiments with carbon black pigment dispersion acting as a Janus ultrasound contrast agent

Jean de Bruin Jordaan, Ken J Nixon, Craig Stuart Carlson, Michiel Postema

BIO Integration

Technical Note

First experiments with carbon black pigment dispersion acting as a Janus ultrasound contrast agent

Jean de Bruin Jordaan[1], Ken J. Nixon[1], Craig S. Carlson[1,2,*] and Michiel Postema[1,2]

Abstract

Background: Theranostic ultrasound contrast agents comprise a therapeutic component whose controlled release is triggered by an ultrasound pulse. However, once the therapeutic component has been released from an ultrasound contrast agent microbubble, its intended uptake cannot be monitored, as its acoustically active host has been destroyed. Acoustic Janus particles, whose hydrophobic and hydrophilic properties depend on the external acoustic regime, are of potential use as contrast agents and drug-delivery tracers. The purpose of this study was to evaluate the hypothesis that submicron particles with Janus properties may act as ultrasound contrast agents whose hydrophobicity changes over time.

Methods: Fifty samples of carbon black were subjected to 5-minute sonication with pulses with a center frequency of 10 MHz and a 1% duty cycle, after which the optical absorption coefficients were measured in *n*-octanol and water. These coefficients were compared with those of unsonicated samples.

Results: Our preliminary results show that the difference between the linear absorption coefficients of sonicated and unsonicated samples was $\Delta\alpha = 80 \pm 13\ m^{-1}$ immediately after sonication, indicating that the carbon black particles were less hydrophobic after sonication than prior to it. Forty-eight hours after sonication, the difference in linear optical absorption coefficients had lessened to $\Delta\alpha = 16 \pm 9\ m^{-1}$, indicating that the carbon black particles had become more hydrophobic over time, but not equal to the hydrophobicity situation prior to sonication.

Conclusion: The experiments confirmed that submicron carbon black particles have acoustic Janus properties.

Keywords

Acoustic Janus particles, hydrophobic contrast agent, optical absorption coefficient, submicron carbon black, transient hydrophilicity.

Statement of significance

The development of theranostic ultrasound contrast agents has been of major interest, especially since the introduction of novel nanomedicines. Such agents cannot be traced after destructive release. Acoustic Janus particles might be used as ultrasound contrast agents as well as drug-delivery tracers. Our finding that submicron carbon black particles have acoustic Janus properties makes them interesting candidates for long-lasting ultrasound contrast agents in theranostics.

[1]School of Electrical and Information Engineering, University of the Witwatersrand, Johannesburg 2050, South Africa

[2]BioMediTech, Faculty of Medicine and Health Technology, Tampere University, Tampere 33720, Finland

*Correspondence to: Craig S. Carlson, BioMediTech, Faculty of Medicine and Health Technology, Tampere University, Korkeakoulunkatu 3, 33720 Tampere, Finland and School of Electrical and Information Engineering, University of the Witwatersrand, Johannesburg, 1 Jan Smutslaan, Braamfontein 2050, South Africa, E-mail: craig.carlson@tuni.fi

Received: March 6 2023
Revised: May 2 2023
Accepted: July 11 2023
Published Online: August 8 2023

Available at: https://bio-integration.org/

Introduction

Theranostic agents are materials that are not only suitable for aiding in diagnostic imaging, but also in therapeutic applications [1]. Owing to recent developments in nanotechnology, theranostic agents have found use more often in combination with diverse imaging modalities [2–5]. Because of the reliability, availability, and price of ultrasound in imaging and therapy [6], numerous studies have been conducted with acoustically active theranostic agents [7–12]. These acoustically active agents comprise drug-charged microbubbles [13, 14], whose payload is released by means of a disruptive ultrasound pulse [15]. The acoustic disruption phenomena of microbubbles have been extensively observed and described [16, 17]. The subsequent uptake of the released therapeutic component is ameliorated in the presence of pulsating microbubbles, owing to transient permeation of biological cells, a phenomenon called sonoporation [18, 19]. Recent findings indicate that hydrophobic particles might have a similar pore-creating effect on cells as microbubbles [20].

https://bio-integration.org **doi:** 10.15212/bioi-2023-0004

compuscript

Once the therapeutic component has been released from a microbubble, its intended uptake cannot be monitored, as its acoustically active host has been destroyed. As it would be highly beneficial to monitor drug uptake for the quantification of treatment efficacy, there might be a demand for theranostic agents that remain acoustically active after drug release.

A futuristic approach would be to create a drug surrounded by a gas shell that is to be disrupted following a high-amplitude ultrasound pulse to release the drug, only to grow back after a certain time. If we assume that such a gas shell can only be created if the drug is in a hydrophobic state, and that removal of the gas shell is similar to creating a hydrophilic state, we may refer to such a drug as a Janus drug, since any particle that exists in a partly hydrophobic and partly hydrophilic state is referred to as a Janus particle [21].

In previous studies, we demonstrated that hydrophobic carbon black was forced to become hydrophilic under sonication [22, 23]. In addition, we characterized the acoustic response from carbon black tattoo ink in tissue and tissue-mimicking media [24, 25].

Figure 1 shows an example of a skin tattoo under sonication. The average grayscale value of the backscattered intensity in a region of interest containing carbon black pigment dispersion was measured during five seconds and was observed to drop compared to a control region. Such sporadic *in-vivo* experimental footage suggesting a change in scattering intensity over time has fueled the hypothesis that tattoo ink may change its acoustic response owing to ultrasound-enhanced changes in its hydrophobicity. To date, the *in-vivo* footage is too rare to provide conclusive scientific evidence in that direction.

We hypothesize that submicron particles with Janus properties may act as ultrasound contrast agents that recover their presonication properties over time. The purpose of this study was to address this hypothesis for carbon black.

Theory

The partition coefficient of a particle sample in an equal mixture of octanol and water defines its hydrophobicity [26]. For small samples, quantifying the concentration in either octanol or water is not straightforward. Therefore, colorimetry is a useful indicator, albeit not for absolute values [27–29].

For light rays travelling through an empty transparent container, the following relation must hold:

$$I_c = I_0\, e^{-A_c}, \tag{1}$$

where I_c is the measured light intensity after having passed through the container, I_0 is the light intensity before entering the container, and A_c is the linear absorption of the container. Let us assume an unsonicated particle sample of interest dispersed in a medium inside the container. For light rays travelling through this unsonicated system, the following relation must hold:

$$I_u(x) = I_0\, e^{-\alpha_u x}\, e^{-A_c}, \tag{2}$$

where $I_u(x)$ is the measured light intensity after having passed through the unsonicated system of thickness x [30], and α_u is the linear absorption coefficient of any sample material of choice. Now, let us assume a sonicated sample of interest dispersed in the medium in the container. For light rays travelling through this sonicated system, the following relation must hold:

$$I_s(x) = I_0\, e^{-\alpha_s x}\, e^{-A_c}, \tag{3}$$

where $I_s(x)$ is the measured light intensity after having passed through the sonicated system, and α_s is the linear absorption coefficient of the sonicated sample material. The change in light absorption from unsonicated to sonicated materials can

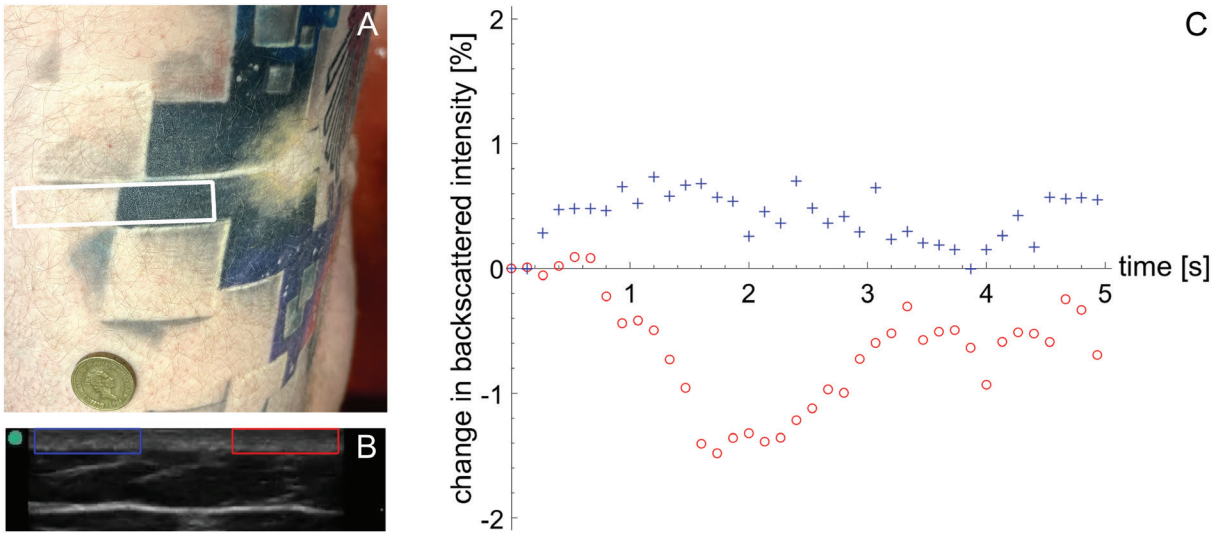

Figure 1 A skin tattoo on the left hip under sonication, with the region of interest containing carbon black marked by a white box (A); a brightness-mode ultrasound image of the region of interest, with the tattooed region indicated by a red box and the control region indicated by a blue box (B); and the change in mean grayscale backscattered intensity normalized by the initial value at time $t = 0$ for the tattooed region (red) and the control region (blue), as a function of sonication time (C).

be experimentally determined by measuring $I_u(x)$ and $I_s(x)$, and by substituting (2) into (3):

$$\Delta\alpha=\alpha_s-\alpha_u=\frac{1}{x}\ln\frac{I_u(x)}{I_s(x)}. \quad (4)$$

If $\Delta\alpha$ is positive, the sonicated sample is less hydrophobic than before sonication. In this study, $\Delta\alpha$ was measured as a function of time.

Materials and methods

Ethics

Conflict of interest: CSC and MP are members of the *BIO Integration* editorial board. They were not involved in the post-submission handling or reviewing process of this manuscript. The authors state no other conflicts of interest. Ethical clearance was obtained from the Human Research Ethics Committee (Medical) of the University of the Witwatersrand, Johannesburg (clearance certificate no. M190808 MED19-07-006). Informed consent was obtained from volunteer participants where required. The manuscript was written without the aid of artificial intelligence.

Preparation

For experiments, a commercial product was used that comprises carbon black submicron particles and clusters thereof. This product, Zuper Black pigment dispersion (INTENZE Products, Inc., Rochelle Park, NJ, USA), had been estimated to have a resonance frequency greater than 10 MHz [24]. Throughout the experiments, a 0.25‰ dilution of Zuper Black in reverse osmosis distilled and degassed water (CJ Distribution, Midrand, South Africa) was used.

Figure 2 shows a brightfield microscopy image of a droplet of the diluted dispersion and the size distribution thereof. The wide size distribution includes particles and clusters. These could not be discriminated in brightfield microscopy, hampering any interpretation of the particle and cluster morphology.

A total of 600 disposable plastic cuvettes (Hughes & Hughes Ltd., Romford, Essex, UK) with inner dimensions of $x \times y \times z$ = 9.9 × 9.9 × 42.5-mm^3 were partly filled by adding 1.5 ml *n*-octanol (Hopkin & Williams Ltd, Chadwell Heath, Essex, UK). To a control subset of these, 1.5 ml reverse osmosis distilled water was added. Throughout this study, the contact angles of the fluids within the cuvettes were monitored, to ensure that the surface properties of the cuvette material did not change over time [31].

Colorimetry setup

The sonication part of the experimental setup comprised an AFG 3031B arbitrary waveform generator (Tektronix Incorporated, Beaverton, Oregon, USA) connected to an A-150 55-dB linear power amplifier (ENI Technology, Inc., Rochester, NY, USA), which was in turn connected to a custom-manufactured single-element very broadband transducer (Neoety AS, Kløfta, Norway) that had been pre-calibrated to generate acoustic amplitudes corresponding to a mechanical index <0.03 at a 10-MHz center frequency. The transducer was positioned along the length axis of a degassed water-filled Perspex container with inner dimensions of 580 × 235 × 65 mm^3, and was held in place by a custom-printed housing of polylactic acid (Ultimaker BV, Utrecht, Netherlands). A custom-printed cuvette housing (Ultimaker) was permanently positioned at a distance of 10 mm from the transducer face.

The photography part of the colorimetry setup comprised an FCL-22CW 8″D Fluorescent Circular Tube (Galaxy Lighting & Brass Ltd., Richmond, BC, Canada) positioned 50 cm above and tilted toward a Mondi Rotatrim white non-creasing paper background (Mondi, Bedfordview, South Africa). A custom-printed cuvette housing (Ultimaker) was positioned between the background and a LifeCam

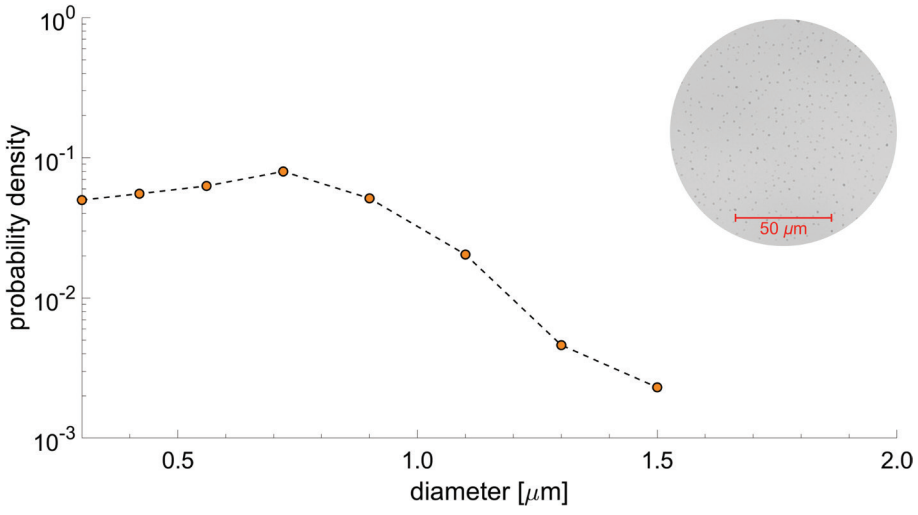

Figure 2 Size distribution of carbon black pigment dispersion and a 63× magnification brightfield microscopy image inlay.

HD-3000 webcam (Microsoft Corporation, Redmond, WA, USA) whose complementary metal-oxide semiconductor had dimensions of 1280 × 720 pixels. The webcam was connected to a laptop computer for camera control and offline image processing.

A schematic line drawing of the experimental setup and some parameters of relevance is shown in **Figure 3**.

Throughout the experimental procedure, a Cartesian coordinate system was used, where the positive *x*-axis was defined as the direction of light in the horizontal *xy*-plane from a point of origin on the background through the cuvette housing.

Colorimetry procedure

A cuvette with pigment dilution was placed in the water-filled container. A pulsed signal was generated. Each pulse was composed of a 100-cycles sine wave with a center frequency of 10 MHz. The pulse repetition rate was 1 kHz, which corresponded to a duty cycle of 1%. Sonication continued for 5 minutes, after which the cuvette was removed from the container. A 1.5-ml sample of dilution was pipetted from the sonicated cuvette into a cuvette with octanol. This cuvette was placed on a PSS 200 AC Orbital Sander (Robert Bosch GmbH, Gerlingen-Schillerhöhe, Germany) operating at 400 Hz for 10 s, before being allowed to settle in the cuvette holder of the photography part of the experimental setup. Photographs were taken at 2.5 minutes (2′30″), 5.0 minutes (5′00″), 7.5 minutes (7′30″), and 48 hours (48°00′00″) after positioning, with a dedicated program written in MATLAB® (The MathWorks, Inc., Natick, MA, USA).

For controls, this procedure was performed as described above, just with the ultrasound transducer physically disconnected from the amplifier. In addition, controls were performed on cuvettes with a mixture of octanol and water only, without pigment dispersion.

This procedure was performed five times with a total of 12 cuvettes in parallel, thus generating five unique datasets, each under constant lighting conditions.

Image processing

Image processing was performed with a dedicated onan procedure written in MATLAB®. Photographs were stored offline in portable network graphics format. Each photograph was converted to a grayscale matrix I_{ij}, which was cropped to exclude all areas outside the region of interest in the cuvette. For each individual pixel in the aqueous phase in the sonicated cuvettes, the grayscale value was compared with the mean value for the corresponding unsonicated cuvette, after which the absorption coefficient difference was computed using equation (4). From these 17280 individual values across five datasets, means and standard deviations were determined [32].

Phantom experiments

Phantom experiments were performed in a setup previously described *in extenso* [24]. In brief, a tissue-mimicking phantom receptacle was constructed with a cylindrical well 40 mm in diameter. The well was filled with undiluted Zuper Black pigment dispersion. The HFL38 13–6-MHz linear probe of a SonoSite® M-Turbo® sonography device (FUJIFILM SonoSite, Inc., Bothell, WA, USA), operating at a mechanical index of 0.6, was clamped to the phantom outer wall.

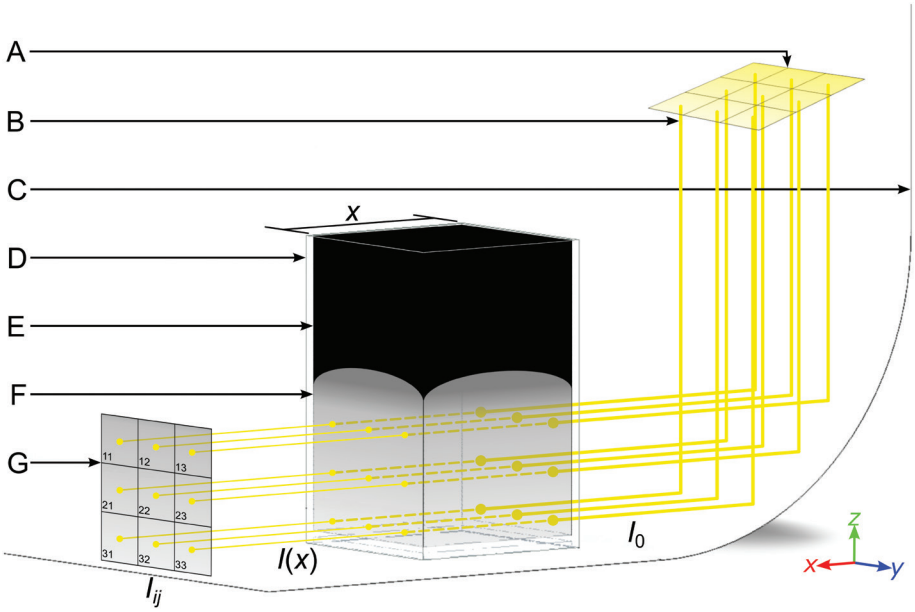

Figure 3 Schematic line drawing of the photography part of the experimental setup, composed of a light source (A) that generated rays of light (B) of intensity I_0 that scattered off a white background (C), passed through a cuvette of thickness *x* (D) containing *n*-octanol (E) and distilled water (F), exited the cuvette with intensity $I(x)$, and were projected onto the complementary metal-oxide semiconductor of a webcam (G) and converted to a grayscale matrix of intensity values I_{ij}. The custom housing of the cuvette is not shown.

Brightness-mode still frames were collected during sonication. The backscattering intensity inside the well was measured as a function of time by averaging pixel grayscale values inside the brightness-mode area representing the inside of the well. For controls, grayscale values representing the phantom material were measured as a function of time.

Results and discussion

The measured contact angles of the *n*-octanol–water interface were found to remain at 26 ± 1° throughout all experiments with pigment dispersion. Thus, the acoustic treatment of the minute quantities of pigment dispersions used in this study had no effects on the surface properties of the dilutants used.

Before elaborating on the quantitative results, we present a qualitative example of changing hydrophobicity due to sonication. **Figure 4** shows representative photographs of unsonicated and sonicated dispersions in cuvettes at 2′30″ after mixing and 48°00′00″ after mixing.

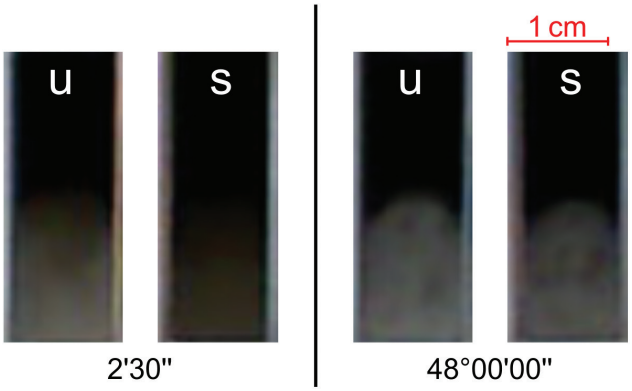

Figure 4 Representative close-up frames of photographs of unsonicated (u) and sonicated (s) dispersions in cuvettes containing *n*-octanol (top) and distilled water (bottom), 2′30″ after mixing (left) and 48°00′00″ after mixing (right). Times are shown below each set of frames.

The light through the octanol phases of all cuvettes was blocked, indicating that they contained hydrophobic dispersion. At 2′30″ after mixing, the sonicated dispersion was observed to be better dispersed in the aqueous phase than the unsonicated dispersion. Thus, a small but non-negligible portion of the pigment dispersion had become hydrophilic.

At 48°00′00″ after mixing, the sonicated dispersion was almost, but not entirely, as clear as the unsonicated solution. This finding indicates that only a fraction of the hydrophilized pigment dispersion remained hydrophilic, whilst the remainder had become hydrophobic again, as it had been before sonication.

Quantitative results are presented in the form of grayscale intensity histograms as a function of time, for all sonicated cuvettes combined and for the unsonicated controls. **Figure 5** shows these intensity histograms at four timestamps after mixing. Immediately after mixing, the histogram of the sonicated samples was farthest left on the *x*-axis, at a position corresponding to the darkest grayscale intensity values. Over time, the histograms of the sonicated samples shifted to the right side of the *x*-axis. The histograms of the unsonicated controls were positioned on the far right of the *x*-axis, which corresponded to the brightest grayscale intensity values. After 48 hours, the histogram of the sonicated samples remained further left than that of the unsonicated controls. This finding indicates that most of the particles that lost their hydrophobicity after sonication had regained it over time. However, as the mean intensity remained below that of the controls, a straightforward explanation may be that some particles lost their hydrophobicity more permanently during the sonication process.

The means of the data shown in **Figure 5** were used for computation of the absorption coefficients using equation (4). The differences in absorption coefficients between unsonicated and sonicated dispersions as a function of time $\Delta\alpha(t)$ are shown in **Figure 6**.

The mean values of all data measured at set time intervals were $\Delta\alpha(2'30'') = 80 \pm 13\ m^{-1}$, $\Delta\alpha(5'00'') = 76 \pm 9\ m^{-1}$, $\Delta\alpha(7'30'') = 53 \pm 17\ m^{-1}$, and $\Delta\alpha(48°00'00'') = 16 \pm 9\ m^{-1}$.

These findings indicate that the carbon black particles became more hydrophobic over time, but did not reach the hydrophobicity observed before sonication. Thus, some

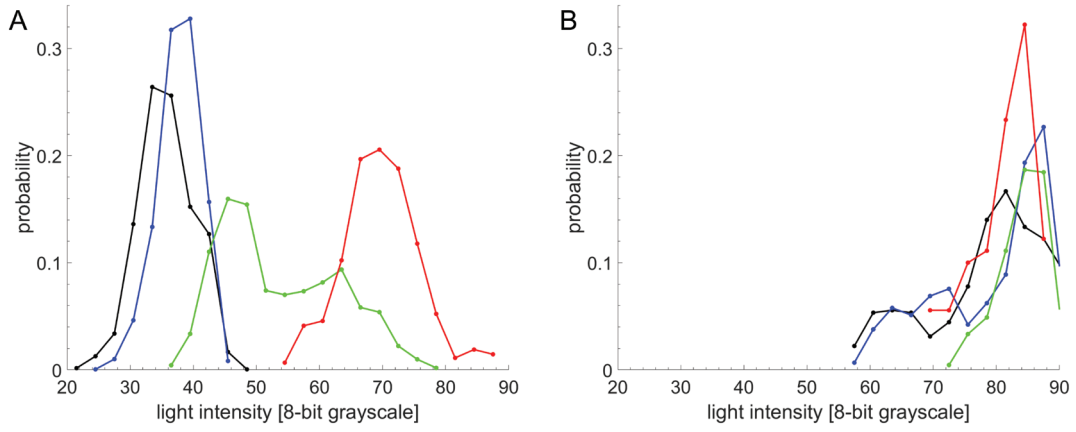

Figure 5 Intensity histograms of light rays that passed through the aqueous phase of the cuvettes at 2′30″ (black), 5′00″ (blue), 7′30″ (green), and 48°00′00″ (red) after mixing, for sonicated pigment dispersion (A) and unsonicated controls (B).

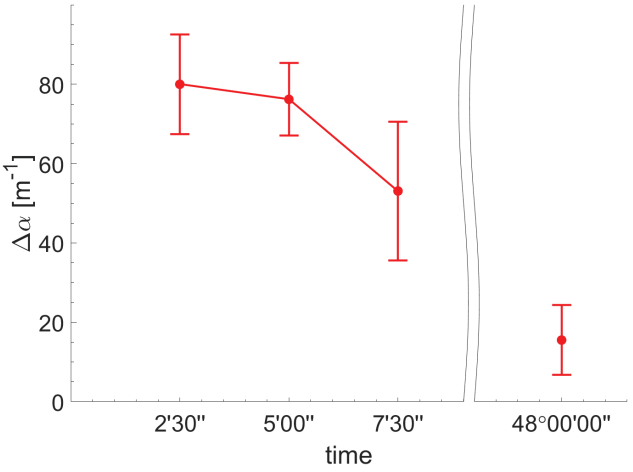

Figure 6 Mean differences in absorption coefficients between unsonicated and sonicated dispersions $\Delta\alpha$, as a function of time.

particles remained hydrophilic after sonication, whilst others became hydrophobic again.

This outcome has proven the existence of Janus particles in pigment dispersion.

Furthermore, an effect of ultrasound on the hydrophobicity of initially hydrophobic particles has been experimentally confirmed.

The colorimetry methodology used in this study resulted in absorption coefficient differences with standard deviations between 12% and 56%. Despite these large errors, the measured $\Delta\alpha$ values could be considered significantly different. Any differences in absolute values between sets of vials may be explained by minute differences in ambient lighting conditions varying between experiments.

In the previous part of this study, we used very low acoustic amplitudes to prevent any unwanted mixing effects from inertial cavitation. In addition to these experiments, we performed experiments at higher-amplitude sonication using commercial clinical ultrasound equipment. **Figure 7** shows the grayscale intensity of brightness-mode ultrasound images from a tissue-mimicking phantom receptacle with a cylindrical well filled with undiluted pigment dispersion. The backscattered intensity was observed to drop compared to the backscattered intensity of the surrounding phantom tissue. This preliminary dataset supports the hypothesis that the hydrophobicity of pigment dispersion may change over time as a result of sonication.

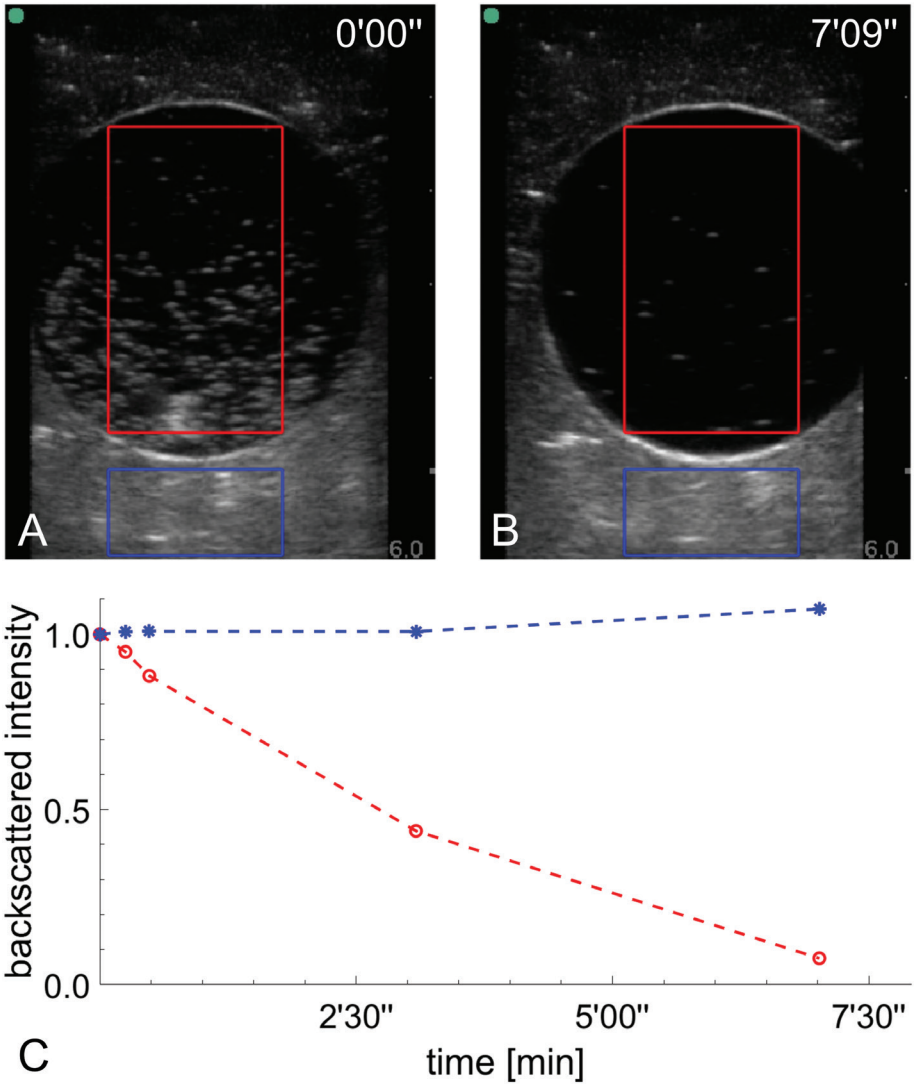

Figure 7 Normalized mean grayscale backscattered intensity of brightness-mode ultrasound images (A, B) of a tissue-mimicking phantom receptacle with a cylindrical well filled with undiluted pigment dispersion, as a function a time (C). Timestamps are shown at the top right.

Conclusions

The experiments confirmed the existence of submicron carbon black particles with acoustic Janus properties.

The instantaneous hydrophobicity could be influenced by sonication at a low acoustic amplitude. However, a minute fraction of the particles remained hydrophilic after sonication.

Acknowledgements

This study was supported by the National Research Foundation of South Africa, grant Number 127102, and by the Academy of Finland, grant Number 340026. A part of this study was included in a dissertation [33]. The sonography device was kindly supplied by High Tech Medical, Randburg, South Africa.

References

[1] Chen X. Integrin targeted imaging and therapy. Theranostics 2011;1:28-9. [PMID: 21499413 DOI: 10.7150/thno/v01p0028]

[2] Lukianova-Hleb EY, Oginsky AO, Samaniego AP, Shenefeldt DL, Wagner DS, et al. Tunable plasmonic nanoprobes for theranostics of prostate cancer. Theranostics 2011;1:3-17. [PMID: 21547151 DOI: 10.7150/thno/v01p0003]

[3] Bhirde AA, Liu G, Jin A, Iglesias-Bartolome R, Sousa AA, et al. Nanotubes for theranostic applications. Theranostics 2011;1:310-21. [PMID: 21769298 DOI: 10.7150/thno/v01p0310]

[4] Tang H, Guo Y, Peng L, Fang H, Wang Z, et al. In vivo targeted, responsive, and synergistic cancer nanotheranostics by magnetic resonance imaging-guided synergistic high-intensity focused ultrasound ablation and chemotherapy. ACS Appl Mater Interfaces 2018;10:15428-41. [PMID: 29652130 DOI: 10.1021/acsami.8b01967]

[5] Tian H, Zhang T, Qin S, Huang Z, Zhou L, et al. Enhancing the therapeutic efficacy of nanoparticles for cancer treatment using versatile targeted strategies. J Hematol Oncol 2022;15:132. [PMID: 36096856 DOI: 10.1186/s13045-022-01320-5]

[6] Huang P. An integrated approach to ultrasound imaging in medicine and biology. BIO Integration 2020;1:105-9. [DOI: 10.15212/bioi-2020-0036]

[7] Feng Q, Li Y, Yang X, Zhang W, Hao Y, et al. Hypoxia-specific therapeutic agents delivery nanotheranostics: a sequential strategy for ultrasound mediated on-demand tritherapies and imaging of cancer. J Control Release 2018;275:192-200. [PMID: 29474964 DOI: 10.1016/j.jconrel.2018.02.011]

[8] Zhou L-Q, Li P, Cui X-W, Dietrich CF. Ultrasound nanotheranostics in fighting cancer: advances and prospects. Cancer Lett 2019;470:204-19. [PMID: 31790760 DOI: 10.1016/j.canlet.2019.11.034]

[9] Sridharan B, Lim HG. Exosomes and ultrasound: the future of theranostic applications. Mater Today Bio 2023;19:100556. [PMID: 36756211 DOI: 10.1016/j.mtbio.2023.100556]

[10] Batts AJ, Ji R, Noel RL, Kline-Schoder AR, Bae S, et al. Using a novel rapid alternating steering angles pulse sequence to evaluate the impact of theranostic ultrasound-mediated ultra-short pulse length on blood-brain barrier opening volume and closure, cavitation mapping, drug delivery feasibility, and safety. Theranostics 2023;13:1180-97. [PMID: 36793858 DOI: 10.7150/thno.76199]

[11] Qin Y, Geng X, Sun Y, Zhao Y, Chai W, et al. Ultrasound nanotheranostics: toward precision medicine. J Control Release 2023;353:105-24. [PMID: 36400289 DOI: 10.1016/j.jconrel.2022.11.021]

[12] Wang Z, Feng Z, Du F, Xiang X, Tang X, et al. Recent progress in theranostic microbubbles. Chin Chem Lett 2023;34:108137. [DOI: 10.1016/j.cclet.2023.108137]

[13] Suzuki R, Klibanov AL. Co-administration of microbubbles and drugs in ultrasound-assisted drug delivery: comparison with drug-carrying particles. Adv Exp Med Biol 2016;880:205-20. [PMID: 26486340 DOI: 10.1007/978-3-319-22536-4_12]

[14] Kotopoulis S, Lam C, Haugse R, Snipstad S, Murvold E, et al. Formulation and characterisation of drug-loaded antibubbles for image-guided and ultrasound-triggered drug delivery. Ultrason Sonochem 2022;85:105986. [PMID: 35358937 DOI: 10.1016/j.ultsonch.2022.105986]

[15] Postema M, Gilja OH. Ultrasound-directed drug delivery. Curr Pharm Biotechnol 2007;8:355-61. [PMID: 18289044 DOI: 10.2174/138920107783018453]

[16] Postema M, van Wamel A, Lancée CT, de Jong N. Ultrasound-induced encapsulated microbubble phenomena. Ultrasound Med Biol 2004;30:827-40. [PMID: 15219962 DOI: 10.1016/j.ultrasmedbio.2004.02.010]

[17] Postema M, Schmitz G. Ultrasonic fragmentation of microbubbles: a theoretical approach of the flash in flash-echo. Proc Annu Int Conf IEEE Eng Med Biol Soc 2005;27:4023-6. [PMID: 17281114 DOI: 10.1109/IEMBS.2005.1615344]

[18] Postema M, Kotopoulis S, Delalande A, Gilja OH. Sonoporation: why microbubbles create pores. Ultraschall Med 2012;33:97-8. [DOI: 10.1055/s-0031-1274749]

[19] Du M, Li Y, Zhang Q, Zhang J, Ouyang S, et al. The impact of low intensity ultrasound on cells: underlying mechanisms and current status. Prog Biophys Mol 2022;174:41-9. [PMID: 35764177 DOI: 10.1016/j.pbiomolbio.2022.06.004]

[20] Anderton N, Carlson CS, Poortinga AT, Xinyue H, Kudo N, et al. Sonic disruption of wood pulp fibres aided by hydrophobic cavitation nuclei. Jpn J Appl Phys 2023;62:018001. [DOI: 10.35848/1347-4065/acaadd]

[21] Fujii S, Yokoyama Y, Nakayama S, Ito M, Yusa SI, et al. Gas bubbles stabilized by Janus particles with varying hydrophilic–hydrophobic surface characteristics. Langmuir 2018;34:933-42. [PMID: 28981288 DOI: 10.1021/acs.langmuir.7b02670]

[22] Postema M, Matsumoto R, Shimizu RI, Poortinga AT, Kudo N. High-speed footage shows transient ultrasonic nucleation of different hydrophobic particles in suspension. Jpn J Appl Phys 2020;59:SKK07. [DOI: 10.35848/1347-4065/ab7f19]

[23] Carlson CS, Matsumoto R, Fushino K, Shinzato M, Kudo N, et al. Nucleation threshold of carbon black ultrasound contrast agent. Jpn J Appl Phys 2021;60:SDDA06. [DOI: 10.35848/1347-4065/abef0f]

[24] Carlson CS, Deroubaix A, Penny C, Postema M. On the attenuation of ultrasound by pure black tattoo ink. SAIEE Afr Res J 2021;112:24-31. [DOI: 10.23919/SAIEE.2021.9340534]

[25] Carlson CS, Postema M. Deep impact of superficial skin inking: acoustic analysis of underlying skin. BIO Integration 2021;2:109-20. [DOI: 10.15212/bioi-2021-0004]

[26] Sangster J. Octanol-water partition coefficients of simple organic compounds. J Phys Chem Ref Data 1989;18:1111-229. [DOI: 10.1063/1.555833]

[27] Kohl SK, Landmark JD, Stickle DF. Demonstration of absorbance using digital color image analysis and colored solutions. J Chem Educ 2006;83:644-6. [DOI: 10.1021/ed083p644]

[28] Gee CT, Kehoe E, Pomerantz WCK, Penn RL. Quantifying protein concentrations using smartphone colorimetry: a new method for an established test. J Chem Educ 2017;94:941-5. [PMID: 34483361 DOI: 10.1021/acs.jchemed.6b00676]

[29] Šafranko S, Živković P, Stanković A Medvidović-Kosanović M, Széchenyi A, Jokić S. Designing ColorX, image processing software for colorimetric determination of concentration, to facilitate students' investigation of analytical chemistry concepts using

digital imaging technology. J Chem Educ 2019;96:1928-37. [DOI: 10.1021/acs.jchemed.8b00920]

[30] Haynes WM, Lide DR, Bruno T, editors. CRC handbook of chemistry and physics. 97th ed. Boca Raton: CRC Press; 2016. [DOI: 10.1201/9781315380476]

[31] Grate JW, Dehoff KJ, Warner MG, Pittman JW, Wietsma TW, et al. Correlation of oil–water and air–water contact angles of diverse silanized surfaces and relationship to fluid interfacial tensions. Langmuir 2012;28:7182-8. [PMID: 22364481 DOI: 10.1021/la204322k]

[32] Squires GL. Practical physics. 4th ed. Cambridge: Cambridge University Press; 2001. [DOI: 10.1017/CBO9781139164498]

[33] Jordaan JdB. Effect of ultrasound on the hydrophobicity of microparticles. Dissertation. Braamfontein: University of the Witwatersrand, Johannesburg; 2022.